UDC 544.478.01, 544.476.2

DOI: 10.15372/KhUR20170104

Effect of Carrier Phase Conversions on the Thermal Stability of γ- and δ-Alumina Catalysts with Low Palladium Content

R. M. KENZHIN[1], A. A. VEDYAGIN[1,2], A. M. VOLODIN[1], V. O. STOYANOVSKIY[1], E. M. SLAVINSKAYA[1], P. E. PLYUSNIN[3], YU. V. SHUBIN[3], and I. V. MISHAKOV[1,2]

[1]*Boreskov Institute of Catalysis, Siberian Branch, Russian Academy of Sciences, Novosibirsk, Russia*

E-mail: romankenzhin@gmail.com

[2]*Tomsk Polytechnic University, Tomsk, Russia*

[3]*Nikolaev Institute of Inorganic Chemistry, Siberian Branch, Russian Academy of Sciences, Novosibirsk, Russia*

Abstract

The present work is devoted to comparative analysis of the activity and stability of palladium catalysts with low palladium content under conditions of three-route catalysis (CO and hydrocarbons oxidation, and nitrogen oxides reduction). Gamma and delta alumina were used as carriers. Catalysts containing 0.12 % Pd and δ-Al_2O_3 on γ- and δ-Al_2O_3 were prepared by the wetness impregnation method. The resulting samples were studied by physicochemical methods. The forced thermal ageing method was used to assess the stability of catalysts to deactivation processes of the active component of Pd. Ethane hydrogenolysis allowed assessing the dispersion degree of the active component. The highly sensitive methods of electron spin resonance (ESR) and electron spectroscopy of diffuse reflectance (ESDR) were used to study the state of deposited palladium. Testing of the catalytic activity of samples under conditions of three-route catalysis was carried out. As a result, it was demonstrated that phase conversions of an alumina carrier did not exert significant effects on the thermal stability of samples during catalytic rFeactions.

Key words: alumina, palladium, decontamination, phase transformations, stability

INTRODUCTION

Normalization of automobile exhausts becomes more and more severe every day. This determines the development of more efficient and resistant catalytic systems that can be stable under operating conditions in a catalytic converter during its normal functioning. Three-route catalysts are broadly used for simultaneous decreasing hydrocarbons, CO and nitrogen oxides emissions from automobiles with gasoline engines [1–3]. Usually three-route catalysts consist of a monolithic block with a large number of parallel channels covered with a porous material [1]. As a rule, this material is based on combination of Pt and/or Pd and Rh, aluminum and cerium oxides, jointly with various stabilizers, promoters, and modifiers [2]. Commercial catalysts may contain one or several these elements, however, all of them comprise of precious metals and aluminium and cerium oxides in various proportions. Catalytic reactions proceed precisely on particles of precious metals distributed in the secondary coating.

According to the literature [4], the major chemical reactions proceeding during catalytic neutralization of automobile exhausts can be represented as follows:

1. Oxidation:

$2CO + O_2 \rightarrow 2CO_2$

$C_xH_y + O_2 \rightarrow CO_2 + H_2O$

2. Reduction:

$2CO + 2NO \rightarrow 2CO_2 + N_2$

$C_xH_y + NO \rightarrow CO_2 + H_2O + N_2$

$2H_2 + 2NO \rightarrow 2H_2O + N_2$

3. CO steam reforming:

$CO + H_2O \rightarrow CO_2 + H_2$

4. Hydrocarbons steam reforming:

$C_xH_y + H_2O \rightarrow CO_2 + H_2$

where C_xH_y – hydrocarbon.

On the other hand, palladium-containing systems are well known as highly efficient catalysts for a broad range of heterogeneous reactions beginning with fine chemical synthesis and ending with partial or complete oxidation reactions. The idea of using palladium as the sole active component of three-route catalysts attracts particular attention for economic reasons (high cost and deficiency of Rh) and accessibility of clean fuels. Despite the limited activity in NO_x reduction, this metal is very active in CO and hydrocarbons oxidation [3]. It should be noted that the activity of three-route catalysts attracts is substantially decreased when a ratio of air-fuel differs from the optimum value [5].

The efficiency of modern three-route catalysts looks impressive in comparison with catalysts having used three and a half decades ago [2]. Catalysts are now placed in an exhaust collector, where they are quickly heated, which allows saving for the amount of the used precious metal. The catalyst efficiency is controlled by on-board diagnostic systems using two oxygen sensors (one before and one after the catalyst) and computer algorithms that periodically changes the exhaust oxygen content and thus, determines the oxygen capacity of the catalyst. Thus, one could say that improvement levels of three-route catalysts are quite high. Further elaborations in this area will associated with reducing the active component load, as well as to increasing the thermal stability of the carriers used.

The present work is devoted to comparative analysis and the stability of low-percentage palladium catalysts. Gamma and delta alumina are used as carriers.

CATALYSTS DEACTIVATION AND THE ROLE OF CARRIER PHASE TRANSITIONS

Catalyst deactivation expressed in a significant reduction of the reaction rate happens resulting from chemical, thermal, physical, and mechanical processes [6].

Chemical deactivation occurs because of strong chemisorption of certain poisons on the catalyst surface. For automotive catalysts, substances contained in lubricating oils and fuels (P, Pb, Zn, S) are poisons. The chemical deactivation degree is proportional to the amount of an exhaust gas. The cross-sectional area of the catalyst with a high volumetric flow rate is most susceptible to chemical deactivation. In this case, the uniform rate distribution allows reaching uniform chemical deactivation and therefore, the maximum catalyst life time.

Thermal deactivation occurs resulting from several various processes in a temperature region of 800–900 °C or even at lower temperatures depending on the material used. Herewith, a decrease in the specific surface area happens resulting from crystals growth, collapse of the porous structure and chemical transformations of catalytic and non-catalytic phases [7]. The first two processes relate to sintering [8], and the last one – high-temperature solid-phase conversions.

Sintering consist in the loss of the specific surface area of the catalyst resulting from the growth of crystals of both the carrier and active component. In case of applied metal catalysts, a decrease in the active specific surface arises resulting from agglomeration and fusion of small metal crystallites into large [9]. Two different models were offered for the sintering process: atoms migration and crystallites migration. In the first case, metal atoms migrate from one crystallite to another along the surface or through the gas phase by decreasing dimensions of some particles and increasing the others. By the other option, crystallites migrate along the surface, collide, and coalesce.

The following equation usually describes the sintering rate [9]:

$$\frac{\mathrm{d}}{\mathrm{d}t}\left(\frac{S}{S_0}\right) = -k_\mathrm{s}\left(\frac{S}{S_0} - \frac{S_\mathrm{eq}}{S_0}\right)^n$$

where S, S_0 and S_eq are current, initial and equilibrium specific surface areas, respectively, m^2; k_s is the constant rate of ageing, s^{-1}; n is the order of ageing (usually $n = 2$).

As noted earlier, complex physical and chemical phenomena are involved in the sin-

tering process of applied metal catalysts, which complicates understanding mechanical aspects of sintering [9]. Experimental observations demonstrated that sintering is highly dependent on temperature, as well as surrounding gas atmosphere. The sintering rate increases exponentially with temperature. Thus, for example, noble metal sintering becomes significant at temperatures above 600 °C. The catalyst temperature in petrol engines can exceed 1000 °C. The sintering mechanism of small metal particles assumes surface diffusion or mobility of large aggregates at higher temperatures. So called Tammann and Hüttig temperature point out on the temperature, at which sintering begins [10].

The temperature, at which the solid phase becomes mobile, depends on several factors, such as texture, size, and morphology. Sintering processes at high temperatures also depend on the atmosphere. Applied metal catalysts are sintered relatively fast in an oxidizing atmosphere and slower in reducing or inert atmospheres. Sintering can also become accelerated in the presence of water vapours. In addition to temperature, atmosphere and time, the sintering rate depends on several other factors, such as the content of noble metals and the composition of the secondary coating. The presence of special additives, as known, reduces sintering. A barium, cerium, lanthanum, and zirconium oxide improves the stability of γ-alumina in relation to sintering in the presence of a large concentration of water in the exhaust gas.

Solid-state conversions represent the extreme form of sintering occurring at very high temperatures and leading to transformation of one crystal phase to another. Phase transformations usually occur in the secondary coating volume. For example, aluminium oxide has many phases: from porous γ-oxide to non-porous α-oxide that is the most stable phase [11–13]. As a result of temperature impact, carriers undergo phase transformations: from tetragonal γ and δ phases into the monoclinic и and hexagonal α. Herewith, the specific surface significantly decreases, and surface properties change. The implementation of the mechanism of nucleation-growth leads to an increase in the size of crystallites up to 20 nm (γ-Al_2O_3), 150 nm (α-Al_2O_3) [14]. It is noteworthy that since the phase transition occurs in stages, the system homogeneity is violated at certain time moments; embryos of the new phase arise, which causes local deformations.

Calcination of commercial aluminium hydroxide $Al(OH)_3$ (Condea Chemie GmbH, Germany) was used for the preparation of γ-Al_2O_3 and δ-Al_2O_3 in this work. Thermal treatment was carried for 6 h at 720 and 1000 °C, respectively. According to X-ray phase analysis, the carrier calcined at 720 °C contains the pure γ phase (less than 1 %). Photoluminescence spectroscopy technique confirmed the availability of such phases. Thus, the selection of carriers is driven by the fact that γ-Al_2O_3 is a system of homogeneous phase with a developed surface (182 m^2/g), capable of undergoing phase transformations under reaction conditions. The specific surface is significantly lower (110 m^2/g) in case of δ-Al_2O_3, the system has phase granularities, but herewith, phase transitions have already been completed.

Catalysts samples containing palladium were prepared by incipient wetness impregnation of carriers (γ- and δ-alumina). A solution of $[Pd(NH_{3)4}](NO_3)_2$ was used as the active component precursor. The palladium concentration in the carrier was 0.12 mass %. After impregnation of carriers with a solution of the active component, they were dried at 105 °C for 12 h and calcined for 1 h at 400 °C in air.

SELECTION OF SENSITIVE METHODS FOR THE STUDY OF CATALYSTS WITH LOW PALLADIUM CONTENT

Intermediate chemical interactions of reagents with catalysts in heterogeneous catalysis are performed on their surface; therefore, obtaining the information about active surface centres is necessary to understand catalytic reactions mechanisms. The concentration of active centres in many cases can be small, and ESR spectroscopy is one of few physicochemical methods that allow reliably working with such concentrations. This method enables to receive information about the structure and properties of paramagnetic complexes on the surface and determine their concentration. At the same time, active catalysts centres, as a rule, do not have their own paramagnetism and because of this are not directly observed by

the ESR method. Therefore, the method of spin probes is used for their study. It assumes conversion of initially non-paramagnetic surface centres into paramagnetic at the expense of their selective interaction with specially selected probe molecules.

In our previous works [15–17], it was demonstrated that donor centres themselves on the carrier surface played an important part in stabilizing atomically dispersed ion forms of palladium. The term donor centres as applied to the surface of oxide catalysts was introduced in the 60th of the 20th century to describe centres able to reducing molecules adsorbed on them at the expense of single-electron transfer (SET). Adsorption of acceptor molecules on such centres usually leads to their reduction to radical anions. The structure of donor centres is still unknown; however, one may suggest they are tightly bound to basic centres of the surface of oxides and the availability of coordinatively unsaturated oxygen anions.

It turned out that precisely donor-stabilized atomically dispersed forms of palladium had the highest activity in the CO oxidation reaction [15–17]. The concentration of such centers on the aluminium oxide surface is low (less than 1 % of a monolayer), therefore, effects of palladium application ere most clearly apparent with its low (to 0.5 mass %) concentrations. Therefore, the present work compares two samples of 0.12 % Pd/γ-Al_2O_3 and 0.12 % Pd/δ-Al_2O_3 that contain relatively small amounts of palladium. The concentration of applied palladium was confirmed by atomic absorption spectroscopy and X-ray fluorescence analysis. Anion radicals generated resulting from adsorption of acceptor molecules of 1,3,5-trinitrobenzene (TNB, E_a = 2.6 eV) were used to determine the concentration of electron-donating centres on the surface of the systems studied. A $2 \cdot 10^{-2}$ M toluene solution of TNB was used in the work. Samples of TNB before absorption were preliminarily calcined at 170 °C for 10 h to remove water from the surface. Adsorption of TNB was carried out right after fast cooling of the ampoule to room temperature.

An ERS-221 electron paramagnetic resonance (EPR) spectrometer (GDR production) operating in the X-range (ν = 9.3 GHz) was used in the work. The power of the microwave radiation in a resonator is to 200 mW. Weakening of the power of radiation is up to 60 dB. Spectrometer sensitivity at the time constant τ = 1 s was $3 \cdot 10^{10}$ spin/G. The frequency of the microwave radiation and magnetic field was measured using a CHZ-64 frequency meter and a Radiopan MJ-100R magnetometer (Poland). The spectrometer control and analysis of the obtained results was carried out using an IBM compatible computer and EPR-CAD software package developed in the laboratory.

Double numerical integration determined the concentration of paramagnetic particles. The work used 2,2-diphenyl-1-picrylhydrazyl (DPPH) radical ($8.3 \cdot 10^{16}$ spins) and solutions of stable nitroxyl radicals TEMPON of a specified concentration for calibration. Rigid fixation of the sample in resonator cavity enabled to decrease errors in determining relative concentrations of paramagnetic particles. Error defining in most our experiments did not exceed 20 %.

Figure 1 presents typical spectra of TNB anion radicals on the surface of 0.12 % Pd/γ-Al_2O_3 and 0.12 % Pd/δ-Al_2O_3 samples, as well as on appropriate carriers. The effect of palladium application on aluminium oxide is clearly visible. An increase in the concentration of TNB anion radicals was observed in the both cases. Additionally, a change in wave shape was observed in case of samples with applied palladium. All this attest to the fact that applied palladium is probably donor-stabilized and modifies donor centres. Herewith, one can see that

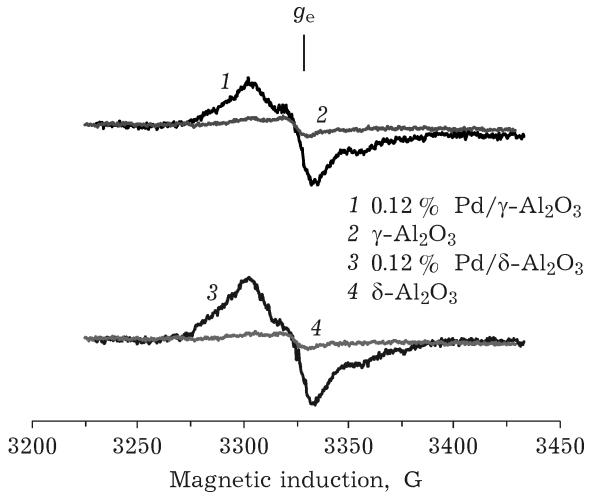

Fig. 1. ESR spectra of TNB radical anions on the surface of various samples: *1* – 0.12 % Pd/γ-Al_2O_3, *2* – γ-Al_2O_3, *3* – 0.12 % Pd/δ-Al_2O_3, *4* – δ-Al_2O_3.

the concentrations of radicals for 0.12 % Pd/γ-Al_2O_3 and 0.12 % Pd/δ-Al_2O_3 samples do not much differ from each other.

One of the factors affecting the activity of applied catalysts is the particle size of the active component. The method of electron spectroscopy of diffuse reflectance (ESDR) in the ultraviolet and visible regions has high sensibility and allows characterizing the condition of applied palladium that is found as Pd^{2+} ions and PdO particles.

The electronic spectrum of applied palladium in the form of isolated Pd^{2+} complexes in the oxygen surroundings consists of a symmetric band at ~22 200 cm^{-1} (~450 nm) corresponding to the spin allowed d–d transition and a ligand-metal $O^{2-} \rightarrow Pd^{2+}$ charge transfer band at 250 nm [18, 19]. The intensity of an adsorption band of d–d transition is proportional to palladium concentration.

The formation of PdO particles leads to band transformation of d–d transition to the absorption edge with a typical value of the width of the forbidden region E_g ~ 2.35 eV.

A shift of the intrinsic absorption edge to the area of large wavelengths is observed in ESDR spectra with increasing an average particle size. The band gap of massive PdO is 0.8–1.5 eV [20]. The typical range of PdO particle sizes, for which the E_g value changes fast enough, is from 1 to 20 nm, which allows using the ESDR method as the Express technique for assessing an average particle size of the active component of palladium catalysts [21, 22].

UV-Vis diffuse reflectance spectra were registered in a range of wavelengths from 200 and 850 nm on a UV-Vis 2501 PC spectrophotometer (Shimadzu) using an IRS-250A set-top box. Appropriate carriers after thermal treatment were used as reference samples under conditions similar to catalysts. Measured UV-Vis spectra were converted to the Kubelka–Munch function $F(R)$ according to the ratio $F(R) = (1 - R)^2/2R$, where R is the experimentally measured reflectance of the sample. The investigated samples were preliminarily calcined in air at a temperature of 600 °C for 6 h. To assess the width of the forbidden zone E_g in the absorption spectra Tauc's plot method was used for the case of direct allowed transitions. The E_g values were obtained by extrapolating the linear section of the spectrum near the low frequency edge of the fundamental absorption band to the intersection with the abscissa axis constructed in the coordinates of $[F(R_\infty)h\lambda]^2$ and $h\lambda$.

Figure 2 presents ESDR spectra of Pd/δ-Al_2O_3 and Pd/γ-Al_2O_3 spectra, as well as absorption edge spectra in Tauc coordinates. From the presented data, it follows that palladium in the initial state is found as isolated forms of Pd^{2+} and PdO small-size particles with close values of E_g ~ 2.26–2.3 eV. Herewith, somewhat smaller average particle sizes of PdO (E_g ~ (2.3±0.01) eV) are typical for Pd/γ-Al_2O_3 in rela-

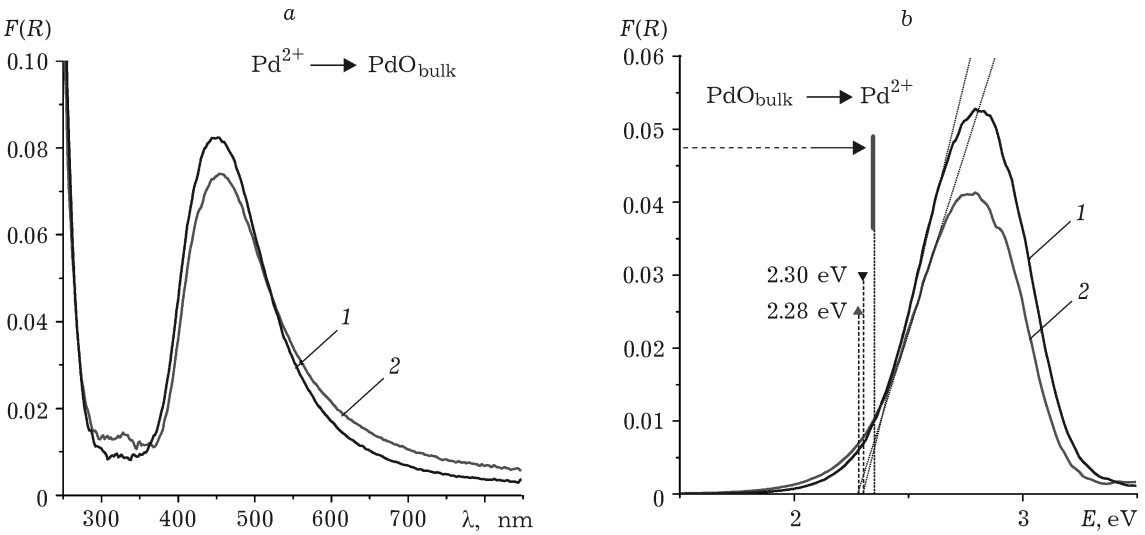

Fig. 2. ESDR spectra of Pd/δ-Al_2O_3 and Pd/γ-Al_2O_3 samples (*a*) and spectra of the absorption edge in Tauc coordinates (*b*): *1* – Pd/γ-Al_2O_3, *2* – Pd/δ-Al_2O_3.

tion to samples on δ-Al_2O3 (E_g ~ (2.26±0.015) eV). Thus, the condition of applied palladium for these two samples is similar.

Ethane hydrogenolysis reference is one more detection method of the concentration of precious metals on the surface of oxide carriers. This method is an alternative to a method of measuring dispersion, according to CO chemisorption, however, has several advantages. The method is based on ethane hydrogenolysis:

$C_2H_6 + H_2 \rightarrow 2CH_4$

The reaction proceeds on metals only and it is sensitive to their insignificant amounts. A characteristic feature of the reaction is that it takes place on each specific metal in a specific temperature range [3, 23]. Thus, for example, for nickel, it is 430 °C, for cobalt − 280−360 °C for ruthenium − 130−180 °C, *etc.* It allows selectively determining dispersion of some metals in the presence of other ones.

All measurements were performed using an automated experimental setup. High-precision threads flows of each of the reaction components are reached using electronic flow regulators. Their use allows varying the mixture composition, according to a specified algorithm and when necessary, completely eliminating one or several components. Gas flows arrive to a heated mixing block that also functions as a preliminary heater. Further, the reaction mixture enters to a quartz reactor, where a sample weight under study is placed. The temperature in the mixing block is specified using thermal regulators also connected to the computer. An analytical part of the equipment consists of a Kristall 2000M chromatograph (Russia) ant two pneumatic crane dispensers that help enter reaction flow samples into a chromatograph for analysis.

The test procedure is relatively simple and looks like follows. A freshly-loaded sample (fraction of about 0.25−0.5 mm, load of 100 mg) is preliminarily reduced in a flow of H_2 at a temperature of 500 °C. To assess the ratio of reduced and oxidized forms of the metal in the initial sample the experiment is carried out twice, moreover, once without preliminary reduction in hydrogen. The reactor is then cooled in a flow of hydrogen to the reaction temperature (200 °C). Further, a flow of helium is mixed with hydrogen and a mixture of H_2/He is let through the reactor for some time until the system reaches the stationary state. Afterwards, ethane is added to the flow. A flow of ethane is let during short time, as a rule, for 3 min. After this, the hydrocarbon delivery is terminated by having preliminarily selected a sample for chromatographic analysis. A mixture of hydrogen and helium is passed through the sample for 10 min during the analysis. This enables to bring the catalyst surface into the initial state. The procedure is repeated 5 times, then the reactor temperature is increased, and repeated kinetic measurements are performed.

The measurement error of conversion in most cases did not exceed 5 % of the absolute value. To process the obtained data experimental points, for which the degree of ethane conversion into methane did not exceed 10 %, were selected. The hydrogenolysis rate (per a gram of palladium) is determined according to the formula $r = (F/W)X$, where F is the ethane feed rate, mol/h; W is mass of metal in a sample weight, g; X is the ethane conversion degree (as a decimal fraction).

Figure 3 presents temperature dependences of ethane conversion in the hydrogenolysis reaction for 0.12 % Pd/γ-Al_2O_3 and 0.12 % Pd/δ-Al_2O_3 catalysts in case of the experiment without preliminary reduction in hydrogen. The maximum ethane conversion at a temperature of 450 °C for the catalyst based on δ-alumina is lower by 0.8 % than for γ-alumina, however, as a whole, the curves are similar. Since the initial reaction rates for the both samples are close, one can suppose that the dispersion degree of applied palladium on samples based

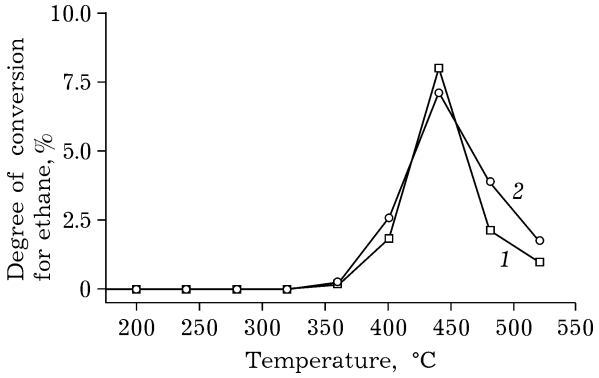

Fig. 3. Temperature dependences of degree conversion for ethane to methane for 0.12 % Pd/γ-Al_2O_3 (*1*) and 0.12 % Pd/δ-Al_2O_3 (*2*) catalysts.

on γ- and δ-alumina are slightly different from each other.

COMPARATIVE ANALYSIS OF THE ACTIVITY AND STABILITY OF PALLADIUM γ- AND δ-Al_2O_3 CATALYSTS

Testing of the catalytic activity of samples under conditions of three-route catalysis (CO and hydrocarbons oxidation, and nitrogen oxides reduction) was carried out using a flow type unit using a QMS-200 quadrupole mass-spectrometer as an analytical cell. Each sample was subjected to 4 heating/cooling cycles. The ratio of air/fuel (λ) for the first three cycles was 1.003, for the fourth one – 0.95. The reactor temperature in each cycle was increased from 100 to 500 °C with a rate of 10 °C/min. The volumetric flow rate was 240 000 h^{-1} with a catalyst charge of 0.250 cm^3. The reaction mixture contained 0.30 vol. % CO, 0.31 vol. % O_2, 0.035 vol. % C_3H_6, 0.015 vol. %, C_3H_8, 0.15 vol. % NO, 10.0. % H_2O, the rest is helium. The stability of samples was studied in a flow type setup under accelerated thermal aging conditions [16, 17]. The reaction flow consisting of 0.15 vol. % CO, 14.0 vol. % O_2 and nitrogen (rest) was fed to the reactor with a rate of 334 mL/min. Each sample was subjected to 7 heating/cooling cycles by varying the final cycle temperature (320 °C for the first two cycles, 600 °C for the subsequent two cycles and 800 °C for the last three cycles). The rate of

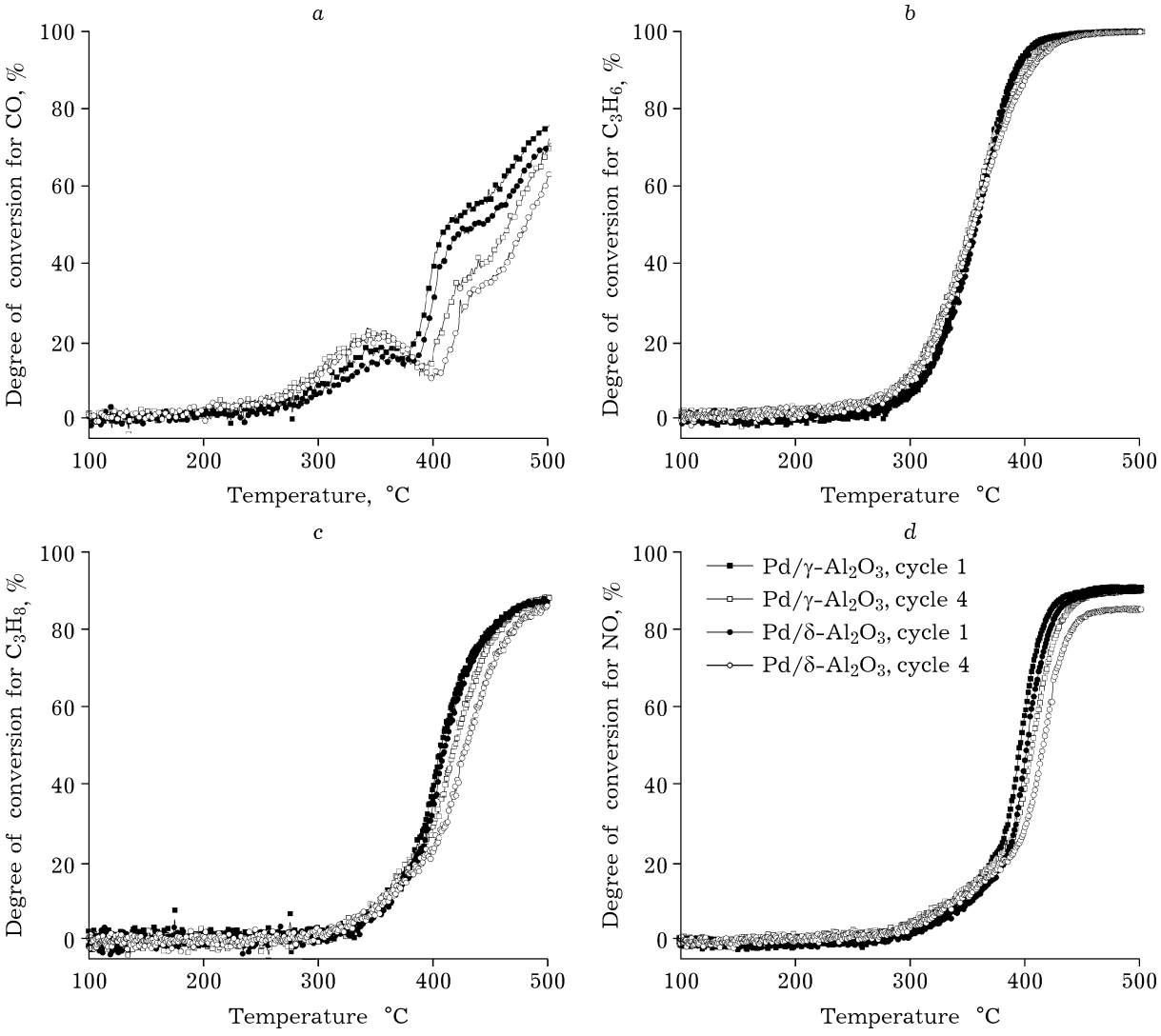

Fig. 4. Temperature dependences of degree conversion for CO (*a*), C_3H_6 (*b*), C_3H_8 (*c*) and NO (*d*) of the first (λ = 1.003) and fourth (λ = 0.95) cycles for 0.12 % Pd/γ-Al_2O_3 and 0.12 % Pd/δ-Al_2O_3 catalysts.

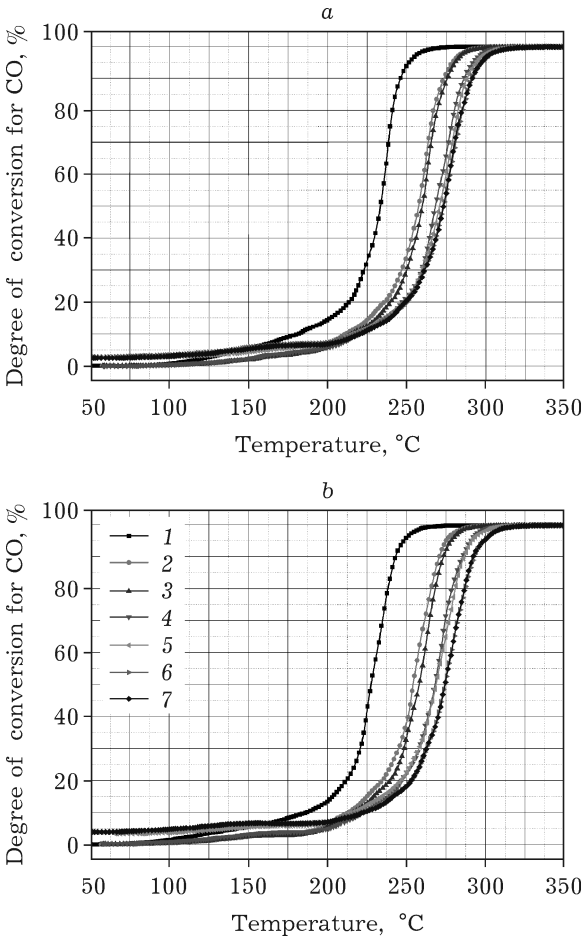

Fig. 5. Temperature dependences of degree conversion for CO in the accelerated thermal aging mode for 0.12 % Pd/γ-Al_2O_3 (*a*) and 0.12 % Pd/δ-Al_2O_3 (*b*) catalysts. *1*–*7* – the heating/cooling cycles with the final cycle temperature 320 (*1*, *2*), 600 (*3*, *4*) and 800 °C (*5*–*7*).

temperature increase in all cases was 10 °C/min. A change in the CO concentration was determined using a Siemens ULTRAMAT gas analyzer.

Figure 4 presents testing results of palladium catalysts based on γ-Al_2O_3 and δ-Al_2O_3 under three-route catalysis conditions, namely, in CO, hydrocarbons oxidation reactions, as well as nitrogen oxide reduction. One can see that the ignition curves for the 0.12 % Pd/γ-Al_2O_3 system almost for all reactions are found 2–5 °C to the left of, in the region of lower temperatures than those for 0.12 % Pd/δ-Al_2O_3. However, as with catalytic studies conducted in the ethane hydrogenolysis reaction, the difference is negligible. Additionally, it is clearly seen that from cycle to cycle curves shifted to the right, towards higher temperatures, which indicates catalysts deactivation. Thus, one can assume that the initial carrier phase condition had little impact on catalysts deactivation process. These data are also confirmed when testing catalysts by the accelerated thermal aging method. This technique allows comparing relative resistance of palladium catalysts to deactivation processes of the active component.

Figure 5 presents data obtained by the forced heat ageing method for Pd/γ-Al_2O_3 and 0.12 % Pd/δ-Al_2O_3 catalysts. It can be seen that the samples are not much different from each other. Oxidation curves shift to the right, to the region of higher temperatures during the subsequent cycles. The catalysts become deactivated, however, the behaviour of 0.12 % Pd/γ-Al_2O_3 and 0.12 % Pd/δ-Al_2O_3 samples is similar. Thus, it can be concluded that carrier phase conversions make an insignificant contribution to catalysts deactivation processes, the major cause of which is surface migration and sintering of palladium particles.

CONCLUSION

Thus, results of studies conducted testify that phase transitions of aluminium oxide do not make a significant contribution to catalysts deactivation processes under three-route catalysis conditions.

REFERENCES

1 Santos H.,Costa M., *AIChE J.*, 57(1) (2001) 218.
2 Twigg M. V., *Catal. Today*, 163 (2011) 33.
3 Vedyagin A. A.,Volodin A. M.., Stoyanovskii V. O., Mishakov I. V., Medvedev D. A., Noskov A. S., *Appl. Catal, B*, 103 (2011) 397.
4 Wang Q., *J. Hazard. Mater.*, 189 (2011) 150.
5 Materials Outlook for Energy and Environment, New Material Science of the 21st Century toward the Solution of Energy and Environmental Issues, NIMS, 2008. URL: http://www.nims.go.jp/eng/publicity/publication/vk3rak0000006o26-att/m_outlook2008.pdf
6 Shim W. G. Jung S. C., Seo S. C., Kim S. C, Catal. Today, 164 (2011) 500.
7 Fernandes D. M., *Catal. Today*, 133–135 (2008) 574.
8 Zhao B., Yang C., Li G., Zhou R., *J. Alloys Compd*, 494 (2010) 340.
9 Shinjoh H., Hatanaka M., Nagai Y., Tanabe T., Takanashi N., Yoshida T., Miake Y., *Top. Catal.*, 52 (2009) 1967.
10 Winkler A., Ferri D., Hauert R., Catal. Today, 155 (2010) 140.
11 Shackelford J. F., Doremus R. H., Ceramic and Glass Materials: Structure, Properties and Processing, Springer Science + Business Media, New York, 2008.
12 Loong C. K., Richardson Jr. J. W., Ozawa M., *J. Alloys Compd*, 250 (1997) 356.

13 Tijburg I. M., De Bruin H., Elberse P. A., Geus J. W., *J. Mater. Sci.*, 26 (1991) 5945.
14 Bowen P., Carry C., *Powder Technol.*, 128 (2002) 248.
15 Vedyagin A. A., Volodin A. M., Stoyanovskii V. O., Mishakov I. V., Medvedev D. A., Noskov A. S., *Appl. Catal. B*, 103 (2011) 397.
16 Vedyagin A. A., Gavrilov M. S., Volodin A. M., Stoyanovskii V. O., Slavinskaya E. M., Mishakov I. V., Shubin Y. V., *Top. Catal.*, 26 (2013) 1008.
17 Vedyagin A. A., Volodin A. M., Stoyanovskii V. O., Kenzhin R. M., Slavinskaya E. M., Mishakov I. V., Plyusnin P. E., Shubin Yu. V., *Catal. Today*, 238 (2014) 80.
18 Gaspar A. B., Dieguez L. C., *Appl. Catal. A*, 201 (2000) 241.
19 Tessier D., Rakai A., Bozon-Verduraz F., *Phys. Chem. Chem. Phys.*, 88 (1992) 741.
20 Okamoto H. and Aso T., *Jpn. J. Appl. Phys.*, 6 (1967) 779.
21 Weber R., Pfefferle L., Luybovsky M., Bozon-Verduraz F., Proc. AIChE Annual Meeting, 1996.
22 Ciuparu D., Bensalem A., Pfefferle L., *Appl. Catal. B*, 26 (2000) 241.
23 Sinfelt J. H., Yates D. J. C., *J. Catal.*, 8 (1967) 82.